Design and Kinematic Evaluation of a 5-DoF Robotic Surgical Instrument

Cameron Crane[1, 4], Nicholas Johannessen[1, 2], Joshua Kleiman[2, 3], Calvin Page[1, 2], Adam Powell[1], Yihao Zheng[1, 2, 4], Sharon Johnson[3], and Sajid Nisar[5]

[1]Robotics Engineering Department, Worcester Polytechnic Institute, Worcester-MA, USA
(Tel : +1-508-831-6665; E-mail: rbe@wpi.edu)
[2]Mechanical and Materials Engineering Department, Worcester Polytechnic Institute, Worcester-MA, USA
(Tel : +1-508-831-5236; E-mail: mme@wpi.edu)
[3]Industrial Engineering Department, Worcester Polytechnic Institute, Worcester-MA, USA
(Tel : +1-508-831-6117; E-mail: business@wpi.edu)
[4]Biomedical Engineering Department, Worcester Polytechnic Institute, Worcester-MA, USA
(Tel : +1-508-831-4112; E-mail: bme-web@wpi.edu)
[5]Department of Mechanical and Electrical Systems Engineering, Kyoto University of Advanced Science, Kyoto, Japan
(Tel : +81-75-496-6343; E-mail: sajid.nisar@kuas.ac.jp)

Abstract: This research presents the design refinement and prototype development of a 5-Degrees-of-Freedom (DoF) robotic surgical instrument for Robot-Assisted Minimally Invasive Surgery (MIS). Instruments with many degrees of freedom and distinct kinematic layouts can operate inside obstructed areas and overcome the limitations of existing solutions. The mechanical and kinematic design of the system is described with considerations for surgical use and prototyped using biocompatible polymer-based rapid prototyping materials. Five DC-motor actuators drive the surgical instrument mounted on pulleys at the distal end, capable of actuating each joint independently through cable-driven transmissions. This work presents the design and validation of mechanisms responsible for achieving actuation in each degree of freedom. Additionally, we implement a teleoperated control system and describe the results and observations of system motion tests. Future work involves improving the design to overcome current limitations and integrating the instrument as an end-effector on a surgical manipulator for future tests.

Keywords: Minimally Invasive Robotic Surgery, Robotic Surgical Instrument, Serial Cable-Driven Robotics

1. INTRODUCTION

Compared to traditional open surgery, Minimally Invasive Surgery (MIS) allows for expedited patient recovery by reducing patients' postoperative trauma [1]. However, operating through small opening incisions on the target area demands high technical precision and dexterity. Specially designed robotic surgical instruments offer surgeons the means to execute Minimally Invasive Robotic Surgery (MIRS), which offers several benefits compared to MIS, especially traditional surgical methods.

First, the smaller entry incisions required by MIRS and MIS, compared to traditional surgical methods, offer many benefits. The smaller the incision, the less bleeding and pain experienced by the patient [1]. These characteristics lead to generally faster recovery times [2], reducing healthcare costs for the patient and operating costs for the hospital. Next, performing MIRS reduces surgeon fatigue [3]. Instead of standing and performing MIS by hand, surgeons can be seated and teleoperate the robotic surgical instrument. Finally, MIRS offers several precision advantages compared to MIS and traditional surgical methods. Robotic instruments can take advantage of mechanical precision and advanced control systems to minimize vibration and other involuntary movements, improving stability and precision over even a well-trained human hand.

To achieve ample dexterity, researchers have previously proposed various kinematic designs with multiple Degrees of Freedom (DoF) that enable these tools to manipulate tissues obstructed by other organs or obstacles. For example, the Sofie robot [4] has multiple degrees of freedom including roll around the tooltip. However, there are no known systems that offer roll around both the shoulder and the tooltip. The design of this device, building upon research by Nisar et al [5-6], is notable for including rotation around the tooltip (wrist roll) and shoulder. This kinematic layout was selected due to its anticipated proficiency in stitching, mobility and stability compared to existing solutions [3]. This paper describes the design, fabrication and control of the robotic surgical instrument.

2. PROPOSED INSTRUMENT DESIGN

The tool outlined in Fig. 1 and Fig. 2 is composed of two main subsystems, the baseplate and the arm. The baseplate houses the system's electronics and motors, while the arm would be the component of the tool inserted into the body interacting with the work area. Separating the baseplate for the arm has benefits regarding the functional size of the tool, sterilization, and the ability to actuate the tool remotely. The baseplate houses the actuators, electronic components, tensioning systems, and shoulder roll mechanics. The arm contains the mechanical elements needed to move the remaining joints. Containing tensioners and actuators in the distal end allows for optimized arm diameter and more effective sterilization.

Fig. 1 Five DoFs instrument prototype with its unique kinematic layout that includes both shoulder and wrist roll.

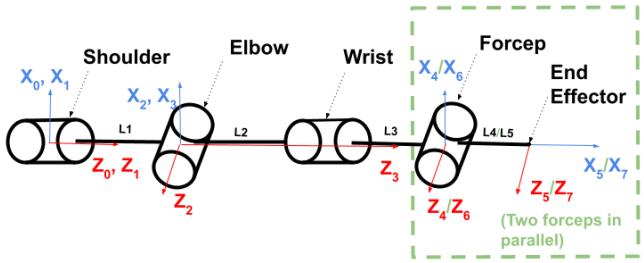

Fig. 2 Kinematic diagram of the instrument.

2.1 Kinematic layout

Fig. 2 shows the kinematic layout of the surgical instrument. The shoulder is attached to the baseplate, which is the end attached to the manipulator. Since the robot uses a forceps tool, and each end of the forceps is controlled independently through an actuator, the system has two end effectors. For simplification, only one side of the forceps is drawn. In practice, the program solves for each end effector position separately. Despite being a 5-DoF system, only 4-DoF need be considered for kinematic analysis. Positions of each end effector are expressed in reference to frame 0, which is the base frame of the surgical instrument.

2.2 Baseplate

The tool has five joints that allow it to achieve its range of motion. These joints are referred to as the shoulder, elbow, wrist, and inner and outer forceps, as shown in Fig. 1. The joints are operated by motors fixed to the bottom of the base plate. The design uses gears to drive the shoulder roll, and tensioned cables to drive the other four joints (Fig. 3). Every motor is equipped with a clamping hub and D-shaft to transmit torque.

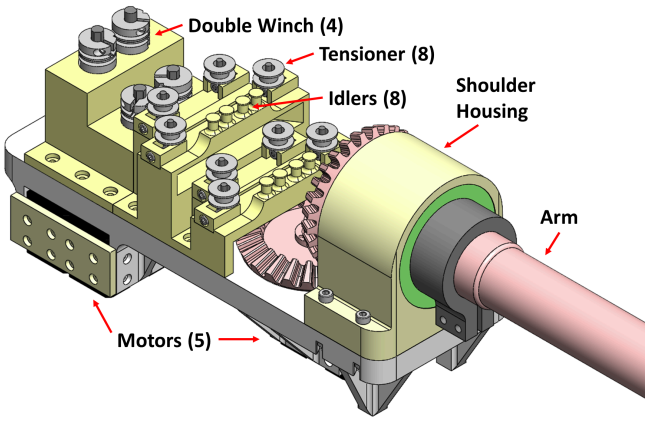

Fig. 3 Isometric view of base plate.

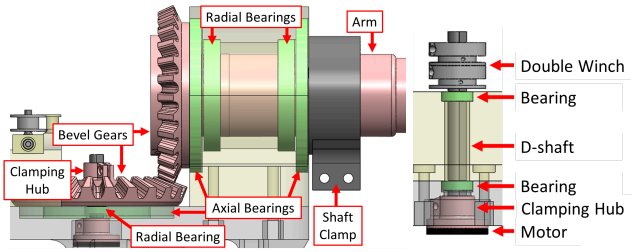

Fig. 4 Side views of shoulder (left) and driving shafts (right)

The shoulder is driven through bevel gears (Fig. 4). The shoulder completes 85.7% of a revolution for every revolution of the driving motor, determined by the ratio of teeth between their two corresponding gears G1 and G2: *G1/G2 = 24/28 = 0.857*. G1 is fixed to its shaft with a clamping hub, ensuring rotational motion from the shaft is translated into the gear. The shoulder is supported by a housing and held in compression with a clamp. Axial bearings are located on either end of the housing to support the axial load, while radial bearings are embedded within the housing to support the radial load.

The other four joints are cable-driven, with each cable's driving shaft being supported by two bearings to handle the radial load. There is also a double winch system clamped at the top of each shaft (Fig. 4). This system allows large magnitudes of tension to be applied on the cables wound in opposite directions around their winches. When the shaft rotates, one spool unwinds while its counterpart winds, increasing tension in one end of the cable and driving the cable loop in that direction. This system also enables each end of the cable to be independently tensioned using their respective tensioner and idler mechanisms. A fully-tensioned system allows for precise cable movement, and therefore, precise actuation of each joint.

Each cable loop passes from the driving shaft to the joint and returns, passing through the tensioning system in both directions. The tensioning system consists of tensioners and idlers for each side of the four cable loops. The tensioner consists of a free-spinning pulley on a dead axle, capable of translating along one axis to adjust the length of the cable loop, and therefore, tension. The idler is used to position the cable to enter or exit the shoulder. Each cable is routed to have its own independent path, unobstructed by other cables or components (Fig. 5). Furthermore, the cables are routed on two different heights to reduce entanglement on the base plate.

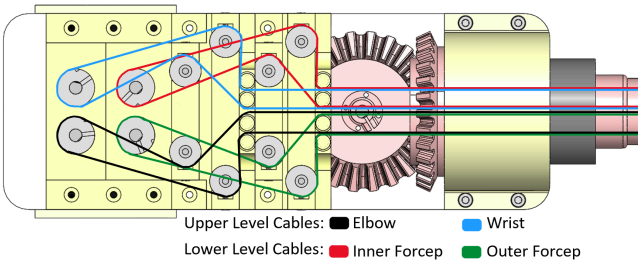

Fig. 5 Cable paths on base plate.

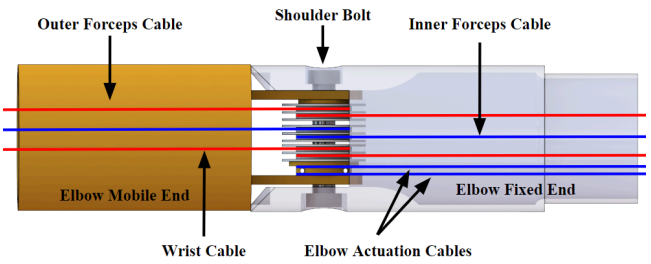

Fig.6 Elbow top down view with transparent fixed end. Pulleys in the center for organization of the cables needed to actuate the wrist and forceps.

2.3 Elbow

The tool controls the pitch of the end effector through the actuation of the elbow joint. The elbow has two main components: the fixed end and the mobile end. The fixed end, depicted in gray in Fig. 6, connects directly to the shaft actuated by the shoulder. The fixed end is secured such that movement of the shoulder corresponds to movement in the elbow. The mobile end connects to the wrist and forceps through a pressure fit. The fixed and mobile ends of the elbow attach with a shoulder bolt located at the proximal end of the elbow's fixed end. The mobile end has radial bearings nested in the extrusions used to fix it to the bolt. Additionally, three free-rotating pulleys with nested bearings are attached to the bolt to assist with tensioning and organizing the cables for the wrist and forceps. These pulleys are each separated by a central wall to have two separate channels to control the location of both halves of the cable responsible for the joint actuation.

Wrapping each cable routed through the elbow around an axle is necessary to maintain tension in the cables for the wrist and forceps. As the elbow moves through its workspace, the cable length needed to actuate the wrist and forceps changes. Wrapping the cables around a central axle fixes the cable length between the base plate and the axle. When the cables wrap around the axle, any additional length change the cable needs will result from winding or unwinding around the pulley while keeping the cable in tension, as depicted in Fig. 7. Having the pulleys and the mobile end rotate about the same axis of rotation limits the amount of string elongation that occurs when the elbow actuates, as no additional offset distance is added to the cable when it moves through its workspace.

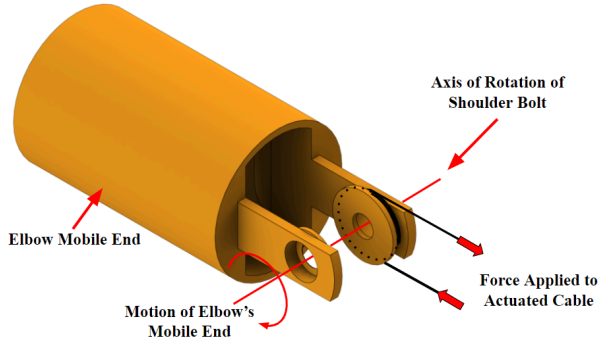

Fig. 7 isometric view of the mobile end of the elbow.

The elbow actuates using cables fixed to the winch embedded in its mobile portion. A single cable is routed through the holes of the winch and secured such that there are cables of equal length on either side of the winch. Each cable is wound in opposite directions around the winch, showing cable tension and its corresponding rotation, thus creating a double winch. When one-half of a cable experiences tension, it imposes torque on the winch. Thus, the elbow rotates in the direction corresponding to the tangential tension force of the cable. The rotation of the winch also causes the other end of the cable to wind in the opposite direction around the winch. The elbow will remain fixed when both cables are in equilibrium and full tension.

2.4 Wrist and forceps

Adopting the ability for a joint's axis of rotation to be collinear with its link surfaces is a fundamental challenge with cable-actuated serial manipulators and adds important capability to a surgical device. On a sufficiently short link (L2 in this case), this motion will rotate, tangle, and elongate any cable loops that traverse the joint in the kinematic chain. In traditional serial manipulators, a slip ring can transmit electricity past such joints in the kinematic chain to power motors or other electronics. However, there is no equivalent to a slip ring to transmit mechanical power through tension force rather than electricity. To solve this issue, the proposed design, depicted in Fig. 8, includes cable loops that terminate before wrist rotation.

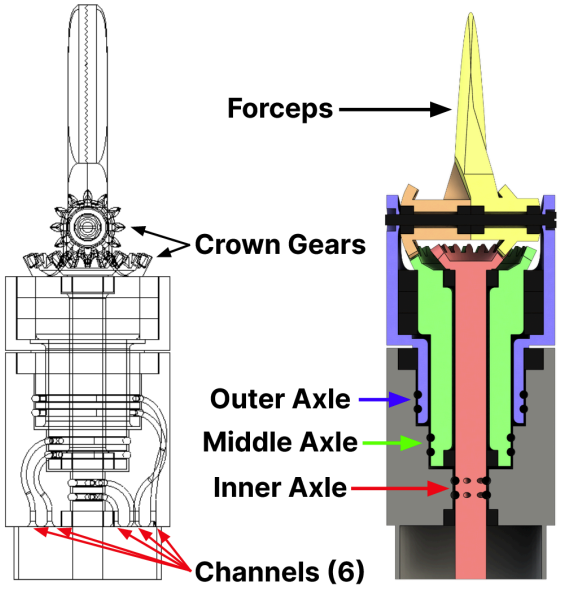

Fig.8 Wireframe side view (left) and cross section front view (right) of wrist roll and forceps.

This design terminates the wrist roll and both forceps' cable loops at the same stage, where they each transmit force to one of three nested axles. The outer axle, as shown in Fig. 8, is the part that holds and rolls the forceps. The middle and inner axles have a crown gear [7] on their opposite ends that mesh with a corresponding crown gear on each of the forceps, enabling their actuation.

This wrist roll and forceps architecture solves the cable loop twisting problem at the expense of introducing interactions with each of these degrees of freedom. As the wrist rolls, it orbits the forceps around their crown gears, actuating them along with the wrist. Fortunately, these interactions are straightforward to compensate for within control code.

Constraints of size, readily available bearings, and the method used to direct each cable to its respective cable loop primarily drove the implementation of the wrist roll and forceps systems. Larger 20mm ID bearings hold both the wrist roll and middle axles in place, despite their nested placement, to reduce part count and keep the design compact. 6mm bearings hold the inner axle to the middle axle and the elbow piece. 2mm bearings facilitate smooth rotation of the forceps.

As seen in the wireframe side view of Fig. 8, channels direct cables from the elbow joint to tangentially join their corresponding double winches on the nested axles. These channels, achieved with resin SLA printing, have a nominal diameter of 1mm and direct each cable to its respective winch.

The bearings, nested axles, and forceps are all fastened by dropping them into the outer axle forceps holder part and sliding a shoulder bolt through the forceps. The shoulder bolt is secured with a captive nut and prevents any parts from sliding out of the assembly while also acting as the axis of rotation for both independently moving forceps.

This proposed design for wrist roll and forceps actuation effectively solves the challenge posed by wrist roll in a cable-actuated arm without compromising functionality or range of motion. Additionally, it can be manufactured with commercially available parts and ensures smooth motion with minimal friction.

3. KINEMATIC MODELING AND CONTROL

3.1 Control hardware & libraries

The robot uses the coreless DYNAMIXEL XH430-W350-R motors to actuate its joints. These motors were selected for their accessibility and low backlash (0.25°). The Robotis OpenCM 9.04 controls the motors with its associated expansion board, the OpenCM 485 EXP. The OpenCM 9.04 platform is favorable for its compatibility with the DYNAMIXEL product system, external power supply to power the motors, and accessible interface with the Arduino IDE. One major advantage of using DYNAMIXEL motors is support from the "Dynamixel2Arduino" library. This library provides tools to control each motor's torque response and kinematics, which are fundamental tools necessary for higher-level control systems.

3.2 Forward kinematic model

Forward kinematic modeling is a useful testing tool due to its ability to analyze each joint's current angular positions and calculate the end effector's pose in the workspace. Using the MATLAB symbolic toolbox, we calculated the homogeneous transformation matrix for the kinematic chain by obtaining intermediate transformation matrices from the D-H parameters in Table 1.

Table 1: D-H Parameters

Link	$\boldsymbol{\theta}$	d (mm)	a (mm)	α
1	$\boldsymbol{\theta}_1$*-90°	L_1	0	-90°
2	$\boldsymbol{\theta}_2$*	0	0	90°
3	$\boldsymbol{\theta}_3$*	L_2+L_3	0	-90°
4/5	$\boldsymbol{\theta}_{4/5}$*-90°	0	$L_{4/5}$	0°

Afterward, the position vector expressions were implemented in C++ so the OpenCM microcontroller could calculate the cartesian positions of each end effector. Eqs. (1) to (3) calculate the cartesian end effector positions, shown with abbreviations for trigonometric functions and joint variables, (e.g. $c_1 = \cos(\boldsymbol{\theta}_1^*)$). While a simple analysis, this model provides the operator with a tool to test the accuracy and precision of system motions.

$$x = c_1 s_2 (L_2+L_3) - L_{4/5} c_{4/5\text{-}90} (s_1 s_3 - c_1 c_2 c_3) - L_4 c_1 s_2 s_{4/5\text{-}90} \quad (1)$$

$$y = L_{4/5}^* c_{4/5\text{-}90} (c_1 s_3 + c_2 c_3 s_1) + s_1 s_2 (L_2+L_3) - L_{4/5} s_1 s_2 s_{4/5\text{-}90} \quad (2)$$

$$z = L_1 + c_2 (L_2+L_3) - L_{4/5} c_2 s_{4/5\text{-}90} - L_{4/5} c_3 s_2 c_{4/5\text{-}90} \quad (3)$$

3.3 Control

To test the robotic instrument, a teleoperated control program was created in C++ to run aboard the OpenCM 9.04 microcontroller. The program offers several different operations and utilities for testing purposes. Most valuable of these are the position control modes. First, a joystick-style motion control mode to step the positions of each joint in small increments. This mode can help the user visually manipulate the instrument into a certain pose. Additionally, the position input control mode prompts the user for a target joint position and then actuates the selected joint to the specified angle. Moving the joints of the robot is the core functionality of the program.

While the DYNAMIXEL libraries facilitate moving the instrument's joints, the program still must model the transmission ratios to each joint, as well as other "compensation" to account for non-independent motion. In the case of the wrist-forceps assembly, the program compensates for the motion of the wrist by moving the forceps' crown gears at the same rate. Preventing relative motion between the forceps' crown gears and the wrist link is critical to avoid undesired position change.

Another place compensation motion is necessary is the elbow. In Fig. 10, the green cable represents one of three that pass through the elbow to drive the forceps and wrist. Despite the idler pulley in the elbow, motion in the elbow still causes the string loop (closed with the pink dashed line for reference) to shift. The amount it shifts, highlighted in red, must be accounted for as motor compensation. Since the program does not use external sensors and instead relies on the motor encoders to measure joint position, the compensation factor is necessary to convert between joint and motor positions while avoiding unwanted motion.

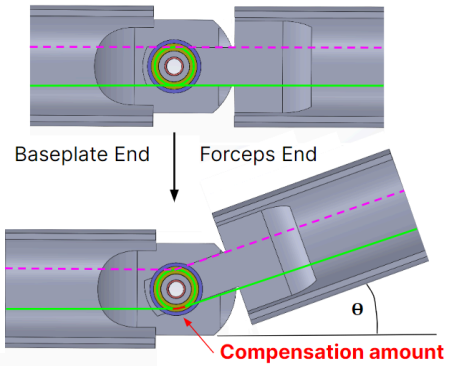

Fig.10 Visual representation of cable length compensation in the elbow joint.

4. EXPERIMENTS AND RESULTS

4.1 Validation

The prototype produced numerous observations to gain insight into the nature of this design. All five joints demonstrated full independent functionality and met or exceeded range of motion expectations.

The shoulder roll is limited only by the number of rotations allowed before the cables are fully entangled and fail. Ten consecutive rotations of the shoulder in the same direction did not limit the functionality of the cables or subsequent joints. The elbow joint rotated accurately up to its mechanical hard stop at around 90 degrees. The wrist roll is limited in its range of motion by the number of winds that can fit within the internal channels on its double winches. The wrist roll demonstrated two full rotations from its prototype. Both forceps are capable of reaching their mechanical hard stops, regardless of the wrist roll's position.

4.2 Individual joint testing

Each degree of freedom underwent individual testing to assess their accuracy. A position θ, representative of the edge of each joint's relevant workspace, was determined. For example, the elbow has a mechanical hard stop at around 90 degrees. Therefore, 80 degrees was selected to sufficiently measure both undershoot and overshoot up to 10 degrees. All joints began their testing by starting at a neutral position in the middle of their range of motion (0 degrees). Then, the joint was commanded to the goal angle of θ, back to 0, to -θ, and finally back to 0. This experiment was repeated five times per joint. The observed angle of the joint at each goal angle was measured to determine the accuracy of the mechanism and software tuning. The value of θ for each joint is as follows:

Table 2: Value of θ in degrees used for testing each joint

Joint	Shoulder	Elbow	Wrist Roll	Outer Forcep	Inner Forcep
θ	180°	80°	90°	80°	80°

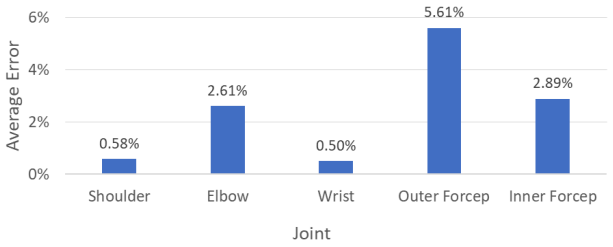

Fig. 11 Average error of each joint.

The results of this testing showed varying accuracy among joints. Fig. 11 communicates the average percentage error between the goal position and the actual position of each joint. The wrist and shoulder demonstrated the highest accuracy, with 0.50% and 0.58% errors, respectively. The elbow and inner forceps displayed lower accuracy, with 2.61% and 2.89% errors, respectively. The outer forceps was the least accurate, with an error of 5.61%.

4.3 Wrist roll compensation

Due to the nested axle design of the forceps and wrist roll mechanism, rotating the wrist requires compensation to ensure the forceps do not change position, as discussed earlier. A grape was placed in the grasp of the forceps, and a 180 degree rotation was commanded. This test, pictured in Fig. 12, was successful; the grape rotated without translating and the forceps maintained a firm grip on the grape.

Fig.12 Wrist roll compensation test with grasp.

4.4 System testing

All five joints were connected and tested using the control algorithms validated previously. When routed around the pulleys in the elbow, the cables responsible for wrist and forceps actuation remained in tension despite the angle of the elbow. The tool had the ability to grasp a grape and manipulate it behind an obstructing object by actuating the shoulder, as seen in Fig. 13. This validated how the tool would distally remove the grape without contacting the obstruction. The tool grasped and moved the grape without releasing or crushing it through its entire motion.

Fig.13 Device manipulating a grape behind an obstacle.

During system testing, a phenomenon was identified in which actuation of the forceps sometimes caused actuation of the elbow. The identified relationship limited the tests of this specific prototype, and potential reasons for this correlation are expanded upon in the discussion.

5. DISCUSSION

5.1 Material limitations

This design was produced entirely with off the shelf nuts/bolts/bearings, fishing line, SLA resin 3D printing, and FDM 3D printing. Although these materials fully enabled the benefits of rapid prototyping and efficient design iteration, their limits led to challenges in testing an instrument intended for surgery. A final surgical device of this nature would be manufactured with metals to overcome these challenges. Beyond material failure of small parts stressed beyond their yield in assembly, one of the largest challenges arose in keeping the device consistently and properly tensioned.

5.2 Design considerations

There are a few factors that potentially led to joints' precisions varying. The control implementation of this device used encoders located within the motors, rather than encoders located on the joints themselves. This required modeling pulley sizes, gear ratios, and link lengths. These values change with manufacturing tolerance and are not rigorously tuned in software. Thus, even small amounts of tuning would drastically impact the performance of any given joint. It is likely that as tests occurred changes in cable length may have occurred due to string elongation or failure of the prototyping materials. Events such as plastic deformation of winches when put under stress may have compromised the prototype, accounting for some of the error found in the results. Steps that can be taken in the future to eliminate this error include integrating encoders on the joints themselves or using computer vision to track joint positions.

Limitations in the prototype materials may cause the relationship between forceps wrist and elbow actuation expressed in the results. During testing, external force applied to the fully assembled and wired elbow resulted in cable slack. One can thus assume that the cable either experienced elongation or the system introduced slack in the cable. From observations, the pulleys likely slipped around the axle when the forceps or wrist introduced a force. If the elbow cannot remain rigid under stress, the tension introduced by the forceps and wrist will be redirected to move the elbow until it becomes rigid. Stronger materials on parts such as the clamping hubs used to transmit torque from axles to double winches would greatly improve if not eliminate many accuracy problems, as these hubs were observed to slip on their axles.

5.2 Considerations for surgical application

Consideration must be given to size, material, and bio-compatibility for surgical applications. While the tool's arm diameter is within the useful range for minimally invasive surgery, miniaturizing the diameter would enable the arm to be used in additional surgery types requiring smaller incisions. Stronger, biocompatible materials that are able to withstand sterilization within an autoclave must be used on any instrument that is used in surgery multiple times. These considerations are extremely important to keep in mind when furthering the development of any aspect of a surgical instrument

6. CONCLUSION

To further the capabilities of MIRS, a prototype 5-DoF surgical instrument with novel kinematic layout is proposed. After being developed in multiple iterations, the motion proficiency of the final prototype was tested to validate the design and identify areas for future improvement. This architecture for a MIRS instrument shows strong promise, offering a compelling alternative to current designs with its distinct kinematic layout.

This 5-DoF robotic surgical instrument aims to eventually lead to improved surgical outcomes. Its enhanced dexterity and ability to work around obstacles hold promise by enabling minimally invasive access to previously inoperable areas, potentially enhancing surgical approaches and reducing reliance on extensive incisions. This translates to faster patient recovery, lower healthcare costs, and a potential for broader societal benefits through improved patient quality of life. While challenges remain in engineering, cost, and regulation, the instrument has the potential to provide another option for minimally invasive robotic surgery and contribute to a healthier society with further development.

REFERENCES

[1] Liu, T. (2010). Design and Prototyping of a Three Degrees of Freedom Robotic Wrist Mechanism For a Robotic Surgery System.

[2] H. Schwaibold, F. Wiesend, and C. Bach, "The age of robotic surgery – Is laparoscopy dead?," Arab J. Urol., vol. 16, no. 3, pp. 262–269, Jul. 2018, doi: 10.1016/j.aju.2018.07.003.

[3] Manger, Charles, Sajid Nisar, Adam Powell (2022). Design and Kinematic Analysis of a 5-Degrees-of-Freedom Robot-Assisted Surgery Instrument

[4] L.J.M. Bedem, van den, "Realization of a demonstrator slave for robotic minimally invasive surgery", *Eindhoven*, 2010

[5] Nisar, S., Hameed, A., Kamal, N., Hasan, O., & Matsuno, F. (2020). Design and Realization of a Robotic Manipulator for Minimally Invasive Surgery With Replaceable Surgical Tools. IEEE/ASME Transactions on Mechatronics, 25(6), 2754–2764.

[6] Hassan, Taimoor, Asad Hameed, Sajid Nisar, Nabeel Kamal, and Osman Hasan. "Al-Zahrawi: A Telesurgical Robotic System for Minimal Invasive Surgery." IEEE Systems Journal 10, no. 3 (September 2016): 1035–45.

[7] McGuire, Patrick, Sprocket and Bevel Gear Generators Website, "https://grabcad.com/library/sprocket-and-bevel-gear-generators-1"